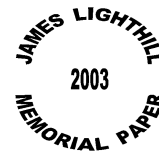# Mathematical modelling of arterial fluid dynamics

TIMOTHY J. PEDLEY

Department of Applied Mathematics & Theoretical Physics, University of Cambridge, Wilberforce Road,
Cambridge CB3 0WA, UK

Abstract. Two major research themes have dominated the fluid dynamical study of blood flow in arteries: (a) propagation of the pressure pulse and (b) flow patterns and wall shear stress (WSS) distribution in complex arterial geometries. The former led to physiological understanding and permitted the interpretation of diagnostic measurements of the wave-forms of blood pressure and flow-rate, for example. The latter was driven by the need to understand the link between wall shear stress and the development of arterial disease, and the understanding gained is also used in the design of surgical interventions such as bypass grafts. Pulse wave modelling has always been essentially mathematical, using one-dimensional linear or weakly nonlinear theory, and can therefore give significant understanding very simply, as is outlined in this paper. The relatively new wave-intensity analysis of the pulse wave shows that the subject is still capable of giving new insight. The study of time-dependent flow in complex three-dimensional geometry, even when the tubes are taken to be rigid and the fluid Newtonian, is much more difficult. Realistic simulation requires the computational solution of the full Navier-Stokes equations, in a geometry obtained from a particular subject by means of magnetic resonance imaging (say), using input flow or pressure data that are also obtained by non-invasive imaging. The combined computational procedure has not yet been developed to the point at which one can have confidence in its accuracy, but it soon will be. However, this is not mathematical modelling and does not clearly lead to new fluid dynamical understanding. For that one must go to idealised models such as uniform curved tubes, which lead to interesting fluid dynamics, but it is not clear how relevant they are to biomedical practice. To show that mathematical modelling is not dead, the paper will conclude with a brief description of a recent model of the new process of transmyocardial laser revascularisation, developed to restore oxygen supply to heart muscle cure off by an infarct, for example.

Key words: arterial fluid dynamics, blood flow, curved tube flow, pulse propagation, transmyocardial laser revascularisation

1. Introduction

In this paper I want to distinguish between *mathematical* modelling and mere computation. If the geometry and motion of a blood vessel and its branches are prescribed, if the inflow and outflow boundary conditions are given and if a simple rheology (*e.g.* Newtonian) is assumed for blood, so that the governing equations (*e.g.* Navier-Stokes) are known, then the full details of the flow can in principle be computed. The output of the computation, in the form of distributions of wall shear stress and pressure, or predictions of the mass transport to the wall of biologically important molecules, may represent a useful contribution to biomechanical science, but that does not make it a mathematical model. Nor is it likely to be a significant contribution to fluid mechanics, unless it reveals or aids the physical understanding of a novel fluid mechanical phenomenon. The process of mathematical modelling requires the formulation of a simplifying hypothesis that permits the isolation of a particular physical phenomenon or mechanism of interest, leads to a reduced system of equations that can be solved or at least investigated by mathematical methods (usually of course aided by computation these days),

and enables the scientist to reach conclusions that encapsulate the underlying physics. This is a rather narrower definition of mathematical modelling than is espoused by the authors of most of the papers in this issue of the *Journal of Engineering Mathematics*, but it is one that would have been recognised by Sir James Lighthill. It is important, however, to emphasise that, in applying mathematical modelling or computation to fluid mechanical phenomena in the cardiovascular system, the goal must be to enhance our understanding of that system. Doing either mathematics or computing for its own sake may be satisfying and enjoyable, but it is not good science unless it leads to something new for the biomedical community, or at least for fluid dynamicists.

Sir James Lighthill was a past master at solving physical fluid mechanical problems by mathematical means. He was an immensely powerful and prolific applied mathematician who could give complete solutions to problems of great complexity, faced with which many other people would simply give up or, these days, put the whole thing on a computer and learn little. However, guided by his aeronautical research in the Second World War which he had to be able to explain to non-mathematicians, he always tried to set out his theoretical ideas in words as well as, or sometimes instead of, equations; this made following the theories somewhat harder for the mathematically trained, but a lot easier for everyone else (see [1] for some examples of his style).

Lighthill did not publish many papers on cardiovascular fluid dynamics but one of them, at least, is a classic: I refer to the chapter entitled "Pulse propagation theory" in his book *Mathematical Biofluiddynamics* [2, Chapter 12]. This chapter provides a concise but admirably clear exposition of the linear, one-dimensional theory of wave propagation in elastic, fluid-filled tubes, including the attenuation effects due to blood viscosity and wall viscoelasticity, the amplitude-enhancing effect of vessel taper, and the mechanics of wave reflection and transmission in a multiply-branched vascular tree. Section 2 of the present paper will be based on that chapter (though without repeating it all) and will ask what additional benefits from mathematical modelling of the pulse wave have been or can be achieved, if any. (Actually there are some!)

Lighthill had a major impact on cardiovascular fluid dynamics research through the founding at Imperial College, London, of the Physiological Flow Studies Unit, directed for many years by C.G. Caro (and now subsumed within the new Department of Biomedical Engineering). It was here that Caro and his colleagues formulated and gave arguments for the "low wall shear stress hypothesis" for the initiation of atherosclerosis in arteries [3]. Their work stimulated an enormous amount of research worldwide on arterial fluid dynamics and how mechanical stresses can modify the biological properties of blood vessel walls, research which continues to this day, as witnessed by several papers in the present issue. There is an excellent introduction to this area of research in Lighthill's survey paper on physiological fluid dynamics [4]. Section 3 of this paper will summarise some of this work and will discuss whether mathematical modelling has any further role to play in arterial fluid dynamics.

Lighthill's other venture into cardiovascular fluid dynamics was less distinguished [5]. This was a model of the pressure-driven passage of an elastic capsule (a red blood cell) through an elastic or rigid tube (a capillary) at low Reynolds number. The analysis was brilliant, as usual, but the physical model was flawed by an unrealistic assumption about the capsule's elastic properties and by an uncharacteristic error in the mechanical formulation, as pointed out by Tözeren and Skalak [6]. Nevertheless this work serves to remind us (a) that blood is not a homogeneous, Newtonian fluid and (b) that the microcirculation is a further source of interesting fluid-mechanical problems. It will not be considered further in this paper, however.

The final subject to be discussed in this paper (Section 4) is chosen as a good example of how a new, speculative, medical procedure has given rise to a novel problem in theoretical fluid dynamics, the solution of which has in turn led to a quantitative understanding of conditions in which the procedure could work. The procedure is "transmyocardial laser revascularisation" (TLR) and is intended to restore blood supply to heart muscle that has been cut off by an infarct. The method consists of using a laser to drill small tunnels part way through the ventricle wall from the inside, so that the wall may be perfused directly from the ventricle. A model of how the beating of the heart enhances the oxygen uptake from such tunnels has been developed by Waters [7, 8] and is briefly outlined here since both the procedure and the mathematical model have some particularly interesting features.

2. Pulse propagation in arteries

2.1. BASIC LINEAR THEORY

When the heart ejects a bolus of blood into the already pressurised aorta, the pressure rises further so the vessel, being elastic, becomes locally distended and the blood in it is set into motion. The coupling between the restoring force of arterial elasticity and the inertia of the blood results in a pressure wave propagating along the aorta. When this pulse wave encounters a bifurcation which is not well-matched, *i.e.*, at which there is a marked discontinuity in admittance (the ratio of pressure perturbation to flow rate) it suffers some reflection and only part of the energy is transmitted. In a normal human subject, the bifurcation at the end of the aorta is mismatched, and the presence of a substantial reflected component is held responsible for the main shape changes of the pressure and flow-rate wave forms as they propagate along the aorta: peaking of the pressure pulse and diminution of the flow-rate pulse. An additional, similar (but smaller) contribution to such shape changes comes from the gradual taper of arteries with distance from the heart, a term that encompasses both a reduction in cross-sectional area and an increase in stiffness and hence wave speed. The dissipative action of blood viscosity and of wall viscoelasticity have a small effect on pulse propagation, though a larger one on the flow-rate wave form. Nonlinear effects are also small in normal subjects, since the *speed index*, analogous to the Froude number for shallow water channel flow, has a maximum value of around 0·25 in the thoracic aorta and is smaller more peripherally. All that can be observed is a slight steepening of the wave front in the aorta.

All these features except the last are analysed physically but precisely by Lighthill [2]; more mathematical expositions are given by Pedley [9, 10], among many others. The analysis always begins by considering a uniform elastic tube containing an incompressible, inviscid fluid, perturbed by small, long wavelength disturbances which are governed by three equations: conservation of fluid mass and momentum and a "tube law" $P(A)$ relating cross-sectional area A to local transmural pressure P (simpler versions of Equations (6–8) below). It is a straightforward matter to deduce that the disturbances obey the linear wave equation, showing that they will propagate without change of shape at a predictable wave-speed, c, where

$$c^2 = \frac{A}{\rho} \frac{\mathrm{d}P}{\mathrm{d}A},$$ (1)

evaluated at the undisturbed value of A, and ρ is the fluid density. Rather fortunately for the credibility of theoreticians, the value of c given by (1) together with measured elastic

properties of segments of excised arteries, agrees quite well with measurements of wave speed *in vivo* (5–8 m s^{-1}). The mechanism of pulse propagation is indeed essentially a balance between wall elasticity and blood inertia, as first correctly analysed by Thomas Young [11].

Wave reflection and transmission at a single bifurcation between three elastic tubes containing an inviscid fluid (parent tube 1, daughter tubes 2 and 3) is also easy to analyse on the basis of continuity of pressure and flow rate at the junction. The wave shape is unchanged on reflection and the amplitude of the reflected pressure wave is a multiple β of that of the incident wave, where

$$\beta = \frac{Y_1 - (Y_2 + Y_3)}{Y_1 + (Y_2 + Y_3)} \tag{2}$$

and

$$Y_j = A_j/\rho c_j \tag{3}$$

is the characteristic admittance of tube j, whose wave speed and undisturbed cross-sectional area, respectively, are c_j, A_j. Peaking of the pressure pulse over the last quarter-wavelength of a sinusoidal wave (virtually the whole length of the aorta) is predicted if $\beta > 1$. This is consistent with human data which indicates that c varies continuously along the arterial tree, but that $A_2 + A_3 < A_1$ at a normal iliac bifurcation.

Extending the analysis to the multiple branches of a complete vascular tree is not possible for a general wave form, because the finite length of a particular artery is a different fraction of the wavelength for each Fourier frequency component. However, the extension can be performed for each such Fourier component, and the complete waveform resynthesised wherever necessary. This was impressively demonstrated by M.G. Taylor [12], who showed how, starting from the peripheral end (*e.g.* zero pressure fluctuations in the venules), a complete tree could be built up, junction by junction, to give a prediction of the flow rate wave form given the pressure wave form (or vice versa) at the entrance to the parent vessel, the aorta. Indeed, the frequency dependence of the input impedance of the aorta (the inverse of the effective admittance of the whole system) has for many years been measured, or inferred from measurement, and used by clinical physiologists to diagnose the mechanical state of the vascular tree [13].

Working in the frequency (ω) domain after Fourier analysis also makes it possible to analyse viscous and viscoelastic effects in a straightforward manner. Womersley [14, 15] and McDonald [16] led the way and many others have followed. In large arteries the frequency parameter

$$\alpha = a\sqrt{\omega/\nu}, \tag{4}$$

where a is vessel radius and ν is fluid kinematic viscosity, is large and viscous effects are confined to thin boundary (Stokes) layers at the vessel wall. It follows that the wave propagation analysis that assumes an inviscid fluid gives a good first approximation to predicting the pressure wave form, from which the influence on the flow rate wave form and the (minor) attenuation can be easily predicted. When wall viscoelasticity is included, using measured mechanical properties, further attenuation is predicted. However, this has led to an apparent inconsistency in the standard, linear, frequency-domain analysis and I do not believe that it has yet been resolved. Histand and Anliker [17] introduced trains of small, high frequency (40–150 Hz) pressure waves into the aorta of a dog, in order to measure the attenuation directly.

In accordance with linear theory, they found an approximately constant attenuation rate, k, per wavelength (amplitude decreases like $e^{-kx/\lambda}$, where x is distance and λ is wavelength); the value of k was typically in the range 0·7–1·0. The theory for a viscous fluid predicts $k = 0·03$–$0·07$ for this frequency range, so the remainder of the attenuation was attributed to viscoelasticity. However, direct measurements of wall displacement [18, 19] have led to estimates of the viscoelastic moduli of the wall that also indicate a wave attenuation rate much smaller than observed. An explanation of such discrepancies is still lacking.

In a paper on mathematical modelling one should also not omit reference to Lighthill's [2] clear physical summary of the WKB method for analysing the pulse wave in a tapering tube. The result is that a constant-amplitude, constant-propagation-speed wave of the form

$$p = P_0 f(t - x/c) \tag{5a}$$

is replaced by

$$p = P_0 \left[Y_0/Y(x) \right]^{1/2} f \left[t - \int_0^x \frac{dx}{c(x)} \right] \tag{5b}$$

in a tube in which the characteristic admittance and wave speed c, defined by (3) and (1) respectively, are slowly varying functions of position. Here the term "slowly varying" means that variation occurs over a distance that is long compared with a wavelength. Since the wavelength of the lowest frequency component in the real mammalian pulse is around four times the length of the aorta, the WKB approximation will be of limited validity in practice.

The frequency-domain approach outlined above enables most of the main, linear mechanisms affecting the pulse wave to be analysed simply and hence understood in some depth. For example, it is possible to use the theory very simply to investigate how the pulse wave may change with age. Dr Johannes Soma (personal communication) has made measurements of pressure and flow-rate close to the root of the aorta, and has observed that the delay between the maximum of the flow pulse and that of the pressure pulse increases with age, although the reverse is commonly stated (based on the wave forms at more peripheral sites). Assuming that the main effect of aging is to stiffen the arteries and hence increase the wave speed, a simple calculation in Appendix A explains the observation clearly: it depends on the measurement site being between one-eighth and one-quarter of a wavelength proximal to the aortic bifurcation.

However, as a simulation tool the frequency-domain approach has two drawbacks. The first is that, in order to predict the input admittance of the systemic vascular tree, it is necessary to start in the periphery, working up generation by generation to the aorta, and thus in principle to know the physical properties (length, characteristic admittance and wave speed) of all branches of the tree. It is of course impossible to measure most, or indeed any, of these, except lengths, *in vivo*, so generic data from post mortem studies is used instead. The conclusions tend to be qualitative at best. Moreover, resynthesising pressure and flow rate wave forms at various sites within different large arteries is cumbersome and not transparent to the user. The second drawback of the frequency-domain approach is that it cannot usually be generalised to cases in which nonlinearity is significant, as it certainly is in particular disease conditions, such as aortic valve incompetence which leads chronically to left ventricular hypertrophy and hence to a large ejection velocity and speed index.

2.2. NONLINEAR THEORY AND COMPUTATION

As large-scale computation became more feasible, therefore, many scientists went back to the time-domain approach, in which the propagating wave form is calculated directly from the complete one-dimensional equations of motion. In a fairly general form, these are as follows, where a suffix x or t refers to partial differentiation:

Mass conservation:

$$A_t + (uA)_x = -\Psi(x, t), \tag{6}$$

Momentum:

$$u_t + uu_x = -\frac{1}{\rho}p_x + \tilde{g} - F(A, u, \ldots)u, \tag{7}$$

Tube law:

$$p - p_{\text{ext}} = K(x)P(A, A_t, x). \tag{8}$$

Here $A(x, t)$ is vessel cross-sectional area, $p(x, t)$ and $u(x, t)$ are pressure and velocity averaged across the cross-section, $\tilde{g}$ is the component of gravity directed along the vessel, p_{ext} is the pressure external to the vessel. The unfamiliar term, $\Psi(x, t)$, in the mass equation is put in to represent outflow at branches, so that the equations can be used for a complete arterial pathway, including junctions. The quantity Fu in Equation (7) is a term usually thought of as representing viscous friction (so F would be a function only of A for quasi-steady flow at low Reynolds number) but it also includes *both* departures of the cross-sectionally integrated convective inertia terms from uu_x *and* momentum loss associated with the mass outflow Ψ. $K(x)$ is a measure of the stiffness of the vessel, non-uniform in a tapered tube, while P is a dimensionless function representing the tube law – this includes A_t among its arguments to cover viscoelastic behaviour, and x to allow for an intrinsic variation in the shape of the tube law function, not just in stiffness.

Careful derivation of the x-momentum equation integrated across the cross-section (see [20] for example) shows that the last term in (7) is in fact given by

$$-Fu = -\frac{S}{\rho A}\tau_w - \frac{\Psi}{A}u'_w - \frac{1}{A}\frac{\partial}{\partial x}\int u'^2 \mathrm{d}A,$$

where S is the (x-dependent) perimeter of the tube, τ_w is the viscous wall shear stress averaged around the perimeter, and u' is the difference between the longitudinal velocity and its cross-sectional average, u (so u'_w is the value of u' at the wall, where the fluid flows out). If the velocity profile is approximately flat, except in very thin boundary layers, then taking $u' \equiv 0$ is legitimate, and this is what is commonly assumed.

The above Equations (6–8) are hyperbolic in form, at least if the functions F and P do not introduce too many complications, and therefore can be integrated using the method of characteristics. Numerous authors did so in the late 1960s and 1970s, in order to investigate various aspects of normal pulse propagation as well as the consequence of vascular disease, such as the development of elastic jumps (analogous to shock waves in gas dynamics) in cases of aortic valve incompetence. This paper is not intended as a review of all the relevant literature, but will merely highlight one or two contributions and developments. One of the most complete studies of pulse propagation along the aorta, iliac and femoral arteries was that

developed by Anliker and his colleagues, the results of which are described at length in [21]. The computation was based on measured values of pulse wave speed (1) as a function of x, rather than of $P(A)$, which clearly enhances accuracy. Pulse wave peaking and steepening was accurately simulated, as were the major consequences of wave reflection from the aortic bifurcation.

However, certain findings did not accord with measurement, such as an increase of mean blood velocity with distance from the heart. Some disagreement with observation is inevitable in a model which contains so many idealisations. These included using a quasi-steady (linear or nonlinear) form for the function F. If unsteady laminar flow is assumed, the appropriate friction term has a phase lead over the mean velocity u which tends to $\pi/4$ for a sinusoidal wave at large values of α. Gerrard [22] pointed out that the method of characteristics cannot be used directly in that case, but requires iteration, thereby removing its advantage over computations based on finite-difference methods. The method of characteristics works quite well only because the friction term is very small in large arteries. A similar problem arises when wall viscoelasticity is taken into account, as discussed by Holenstein *et al.* [23].

A more serious difficulty arises in choosing the proper form of the outflow function Ψ and its effect on the momentum equation (7). To be compatible with one-dimensional computations Ψ has to be smoothed out over a longitudinal distance equal to several tube diameters, rather than concentrated at the branch site, which would be represented by a point (therefore Ψ by a delta function) in the one-dimensional approximation. Anliker *et al.* [21] represented Ψ in the form

$$\Psi = \gamma\,(p - p_c)\,\phi(x), \tag{9}$$

where the function $\phi(x)$ is a smoothly varying function and the factor $\gamma\,(p - p_c)$ is included to represent the resistance to flow in the side branches; p_c is capillary pressure and γ is a constant. This form is equivalent to the assumption that the pressure-flow relation is quasi-steady and linear (*i.e.*, inertia-free) in all side branches, which is clearly not the case. Recognising this, other authors (*e.g.* Chadwick [24]) have sought to model the side branches using a complex admittance in place of the constant γ, but as noted above this really requires analysis in the frequency domain since it will be frequency- (and branch-) dependent.

Many authors realised that, instead of trying to smooth out the effect of branches, especially major branches, it would be better to extend the one dimensional model to account explicitly for each branch, concentrated at a point. If the side branches to the main pathway being analysed can be assumed to behave linearly then, as in the smooth approach, their behaviour can be lumped analytically into an effective, complex, input admittance for each branch. Taking this admittance to be constant is equivalent to lumping the side branch and the vessels peripheral to it into a single resistance-inertance-capacitance system, *i.e.*, the traditional zero-space-dimensional Windkessel which, as a model for the whole arterial tree, preceded the one-dimensional models discussed here. However, if the frequency-dependence of the admittance is taken into account, as it should be according to one-dimensional theory, the whole calculation will have to be performed iteratively: direct integration along characteristics is not possible. On the other hand, if the nonlinearity in the branches is as important as in the main pathway, there is nothing for it but to perform the nonlinear, one-dimensional computation separately for each significant branch of the vascular tree, linked by continuity of pressure and flow-rate at each junction.

Among the first full one-dimensional models of the aorta and legs, with lumped, linear side-branches was that by Raines [25], who proved the feasibility of the method. Olufsen [26]

formulated a method for predicting the input impedances of the side and peripheral branches of an arterial tree, the central part of which consisted of three or four generations of branches to be simulated in detail. Her method consisted of supposing that a peripheral bed supplying a certain region of tissue consisted of a number of systematically asymmetric bifurcations for which the frequency-dependent input admittance could be computed analytically. The number of bifurcations would be determined by the size of the region being supplied. The output of her model, albeit still a linear model, showed a much better phase relationship between pressure and flow-rate wave forms than models with constant peripheral admittances.

As the one-dimensional computations have become more or less routine, attention has turned to improving the basic model, especially in the context of abnormalities such as stenoses (constrictions) in one part of the system, or the introduction of bypass grafts, etc. If nonlinearity is important in the one-dimensional equations, then surely it should be important in the matching conditions linking two or three vessels of the system at stenoses or branches? An early investigation is the very simple analysis by Pedley [27] of the reflection and transmission of a linearly propagating pulse wave at a nonlinear stenosis, *i.e.*, one across which the pressure drop is proportional to the square of the flow-rate. Here the nonlinearity requires nothing more complicated than solution of a quadratic equation at each time step. Clearly this analysis could be used as easily for nonlinearly propagating waves.

Much more recently, Sherwin *et al.* [28] have derived the appropriate nonlinear matching conditions at a bifurcation, assuming that there is no energy loss there (in contrast to the stenosis model of Pedley [27]). Flow-rate is of course continuous, but it is total pressure, $p + \frac{1}{2}\rho u^2$, that must also be conserved. The difficulty is to incorporate this boundary condition into a numerical scheme for computing pressure and flow-rate everywhere. The key to doing this came from the recognition that conditions at the branch at a certain time are determined from the incoming characteristics only, that is from the forward-travelling wave in the parent vessel, and from the backward-travelling (reflected) waves in the daughters. This work appears to provide the first rational way of modelling nonlinear wave propagation and reflection in a general branched-tube network, with the branch matching conditions approximated as accurately as the basic wave propagation, as long as there are no significant energy losses at the bifurcations.

However, the flow in complex, three-dimensional geometries does normally give rise to energy losses. Once attention is focussed on the complicated details of what happens at branches, the whole philosophy of the modelling shifts. Instead of treating a junction as occupying a point in a one-dimensional model, the purpose of studying which is to determine the boundary conditions to be applied in that model, Quarteroni and his colleagues are now looking at the detailed three-dimensional flow in the junction, and the one-dimensional models of the arteries that meet there are used to provide the boundary conditions for that study [29, 30]. However, the details of flow in branches is important for other reasons, so discussion of them is postponed to Section 3.

2.3. Wave-intensity analysis

Before leaving the one-dimensional theory of the pulse wave, it is worth summarising a rather different way of looking at it which has led to a new and insightful interpretation of measurements of pressure and velocity wave forms. The method was introduced by Parker *et al.* [31] and that group has since developed it much further [32–35]; others have also joined in [36].

Let us return to the simple, frictionless version of the Equations (6)–(8) for waves in an intrinsically uniform tube, which (using (1)) can be written

$$p_t + up_x + \rho c^2 u_x = 0, \tag{10a}$$

$$u_t + uu_x + \frac{1}{\rho}p_x = 0. \tag{10b}$$

The standard Riemannian theory, in which $\pm\rho c$ multiplied by (10b) is added to (10a), shows that the quantities $p \pm \int \rho c \, du$ remain constant along the characteristic curves $C_\pm$ in x, t space, defined by $\frac{dx}{dt} = u \pm c$; we assume that $|u| < c$ everywhere, *i.e.*, no elastic jumps develop. Any finite wave can be analysed as the sum of infinitesimal 'wavelets', consisting of small increments in pressure and velocity, Δp and Δu. Because every point in x, t space has a C_- characteristic passing through it, on which $p - \int \rho c \, du$ is constant, it follows that, for every forward-travelling $(C+)$ wavelet, the changes in p and u are related by

$$\Delta p_+ = \rho c \Delta u_+. \tag{11a}$$

Similarly for backward-travelling $(C-)$ wavelets,

$$\Delta p_- = -\rho c \Delta u_-. \tag{11b}$$

The *wave intensity* (WI) is defined by

$$WI = \Delta p \Delta u; \tag{12}$$

this is entirely analogous to acoustic energy, as discussed by Lighthill [37]. Hence, since $\Delta p = \Delta p_+ + \Delta p_-$ and $\Delta u = \Delta u_+ + \Delta u_-$, we have

$$WI = \frac{1}{\rho c}\left(\Delta p_+^2 - \Delta p_-^2\right). \tag{13}$$

That is, forward-travelling waves contribute only positively to WI and backward-travelling waves only negatively, whatever the signs of Δp_+ and Δp_-.

Whether the pressure and velocity waveforms in an individual subject are measured simultaneously or are averaged over several cycles, it is easy to divide the cardiac cycle into a number of time intervals, read off Δp and Δu from each interval, and calculate WI from Equation (12). The result is a plot of WI against time throughout the cycle. Figure 1a, from [35], shows pressure and velocity waveforms simultaneously measured in the ascending aorta of a dog under control conditions. The corresponding wave intensity plot is given in Figure 1b. It is remarkable that there are two large positive peaks, just after the aortic valve opens and just before it closes, and only a rather weak negative signal (reflected wave) in between.

A matter of some interest, in the diagnosis of obstructions in arteries or merely in the assessment of the general state of a subject's vascular health, is the separation of the measured waveforms into their forward- and backward-travelling parts. This can be done without further measurement if it is *assumed* that the wave speed is constant at the measurement location. It will be constant if the pressure pulse amplitude is sufficiently small relative to the mean pressure for the wave to behave approximately linearly. Then

$$\Delta p_+ = \frac{1}{2}(\Delta p + \rho c \Delta u) \quad \text{and} \quad \Delta p_- = \frac{1}{2}(\Delta p - \rho c \Delta u) \tag{14}$$
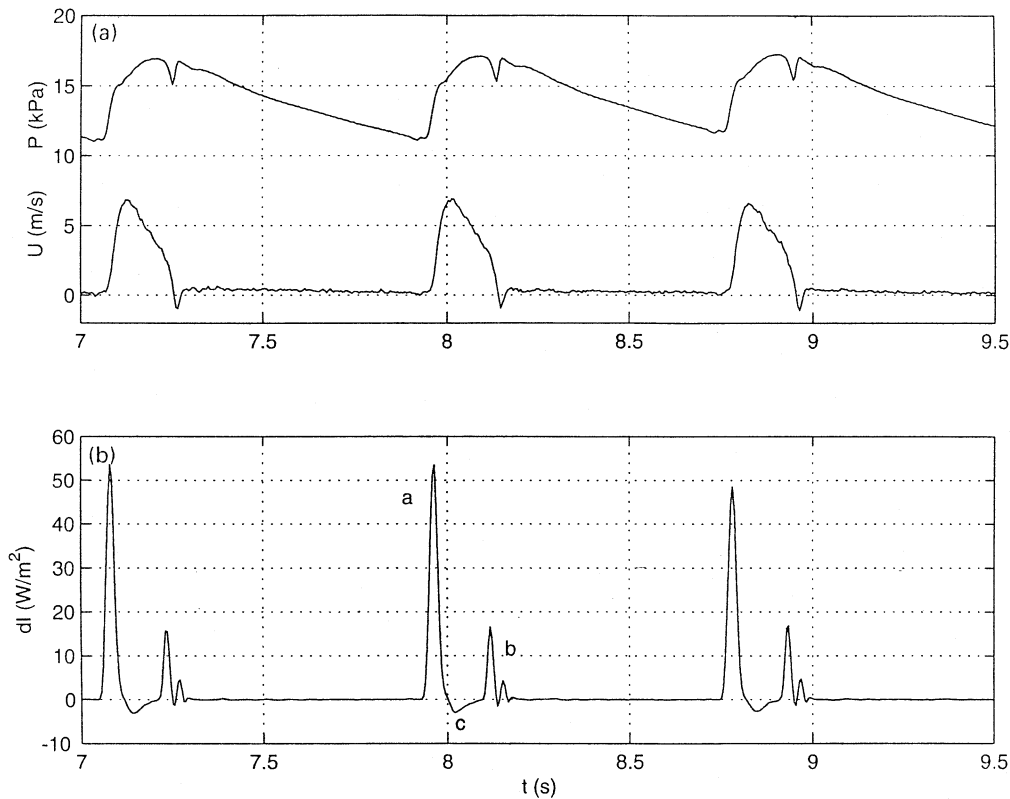
Figure 1. (a) Pressure and velocity as functions of time, measured in ascending aorta of a dog under control conditions. (b) Wave intensity calculated from the data in (a), using equation (12): note a – the initial forward compression wave at the start of systole, b – the forward expansion wave at the end of the systole, c – backward, reflected waves in mid-systole. (From [35], with permission.)

and, if c is known, $\Delta p_{\pm}$ can be calculated. Moreover, c can usually be inferred from a plot of p against u throughout the cycle. Figure 2, also from [35], shows such a p, u loop measured in the ascending aorta of a dog under control conditions and with total occlusion of the upper thoracic aorta. Both curves have a straight line segment, corresponding to the early ejection phase during which one can be safe in assuming that there are no backward-travelling waves in the ascending aorta. The slope of this segment, from Equation (11a), is ρc, from which c can be determined.

Figure 3 shows the wave intensity from Figure 1b separated into its forward- and backward-travelling parts. It can be seen that there is only a small backward-travelling component at any time, though during the long period between the first and the second forward travelling peak there is *only* a rather broad backward-travelling wave. Figure 4 shows the pressure and velocity wave-forms similarly separated. These graphs show an interesting phenomenon during diastole, during which there seem to be equal and opposite, gradually declining, forward- and backward-travelling contributions to the flow velocity, which is zero. These, and the corresponding pressure curves, look like an artefact, but can in fact be interpreted in terms of a gradually-subsiding capacitance, as in the old Windkessel model [38].
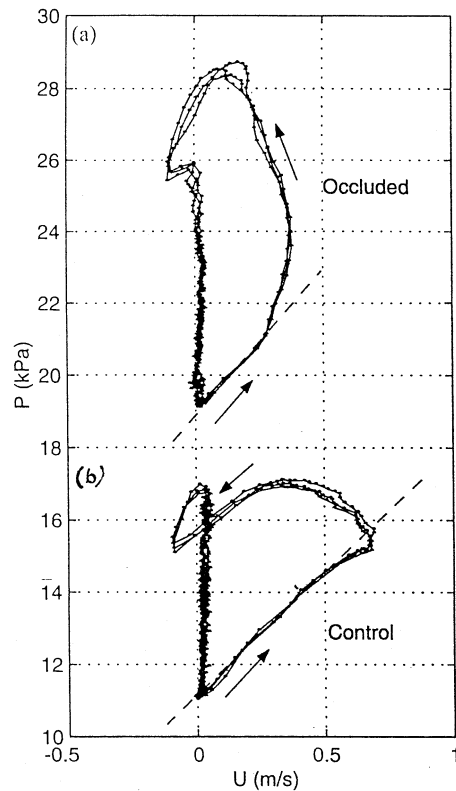
Figure 2. The $p - u$ loop, derived from data sampled at 200 Hz, from the ascending aorta of dogs (a) in which the upper thoracic aorta is occluded and (b) in control conditions. The slope of the dashed line gives the wave speed in early systole, from Equation (11a). (From [35], with permission.)

3. Blood flow in complex arterial geometries

3.1. GENERAL

Prior to the late 1960s, pulse propagation was the only aspect of arterial blood flow that had been subjected to systematic fluid dynamical analysis. At that time, however, the focus of attention switched to measurement and analysis of the detailed flow patterns and distributions of wall shear stress (WSS) within arteries. This came about as a result of two seminal contributions: by D.L. Fry [39], who noted that arterial endothelial cells could be damaged by severely *elevated* levels of WSS, and by C.G. Caro and colleagues [3] who observed a rough correlation between arterial sites which are prone to the development of arterial disease (atherosclerosis) and sites at which the mean level of WSS would be expected to be *low*. This expectation was based on a rather crude view of arterial fluid dynamics, but it has stood the test of time, and the low-mean-shear hypothesis for the initiation of atherosclerosis has largely prevailed over the high-shear hypothesis, although there is evidence that time-dependence of the flow (in the form of repeated flow reversals) also has an effect [40].

The low-shear/high-shear debate was a tremendous stimulus to research in arterial fluid mechanics, as well as in vascular wall biology. The aims of the latter have been to reveal the biological and structural effects of various levels of WSS on endothelial cells (*in vitro* as well as *in vivo*) and to try to understand how they come about (Davies [41]). The aims of
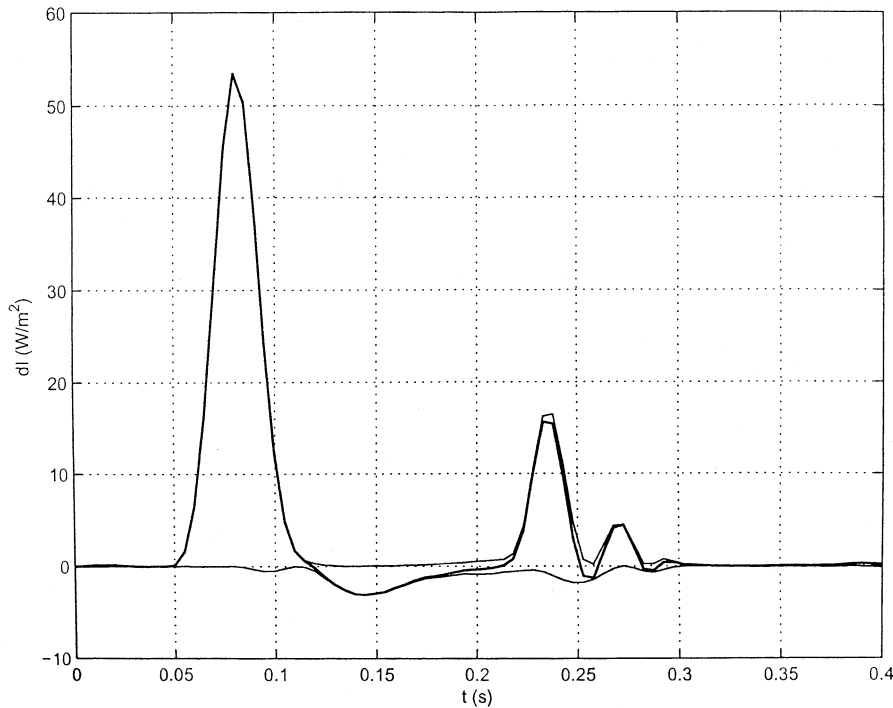
Figure 3. Wave intensity, and its forward- and backward-running components, calculated from the data of Figure 1, using Equations (12) and (14). (From [35], with permission.)

the former are to reveal and understand the actual distribution of WSS in the complex three-dimensional geometry of large arteries. These aims have spawned a huge number of papers in the fluid dynamics and bioengineering literature, describing model experiments, numerical computations and mathematical analysis of the flow in a sequence of increasingly complex geometries representative of normal or diseased arteries and of surgical modifications to them (such as femoral bypass grafts). Topics considered have included: entry flow in straight tubes; flow in constricted tubes; fully-developed and entry flow in uniform curved tubes; flow in helical tubes; flow in moving tubes; flow in symmetric planar bifurcations; flow in asymmetric branches; flow in non-planar curves or branches; flow in all of the above when the vessels are elastic instead of rigid; using non-Newtonian as well as Newtonian models of blood rheology; investigating unsteady as well as steady flow. Since the mean Reynolds number in large arteries is quite large (several hundred, typically) the flow and WSS distribution are extremely sensitive to small geometrical perturbations and to small changes in the time-course, as represented by the wave-form of pressure-gradient or flow-rate. Steady flow can be non-unique, and stable or unstable, though rarely fully turbulent. See [42–45, 9, 10] for reviews and further references.

Such sensitivity to the precise spatial or temporal details raises doubts about the predictive value of many of the numerical or experimental simulations that are performed on (for example) home-made bifurcation models, or even casts of an individual subjects' vessels. They reveal great complexity of flow, which in itself is instructive, but since one subject's complexity is likely to be different from another's, what is to be gained (other than technical expertise) from the quantitative minutiae? In my view, thorough quantitative investigations should be restricted to two extremes of the spectrum.
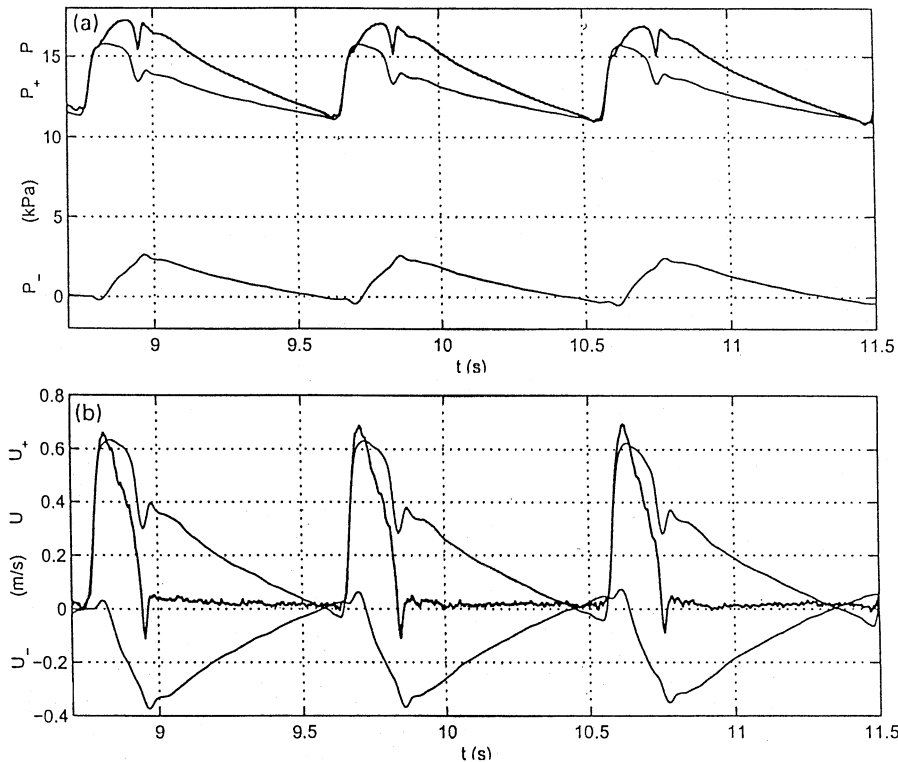
Figure 4. The measured pressure (a) and velocity (b) wave forms, separated into their forward- and backward-running components. (From [35], with permission.)

The first approach, currently being followed by several groups in North America, Europe and Japan, is to seek to simulate the flow in each individual patient and predict the WSS distribution for use in diagnosis or surgical planning (it goes without saying that the direct and accurate measurement of WSS is not feasible using any known technique). This requires direct imaging of the geometry, for example using magnetic resonance imaging (MRI). Then the MR data, "suitably" smoothed (a process about which there is considerable controversy), must be automatically converted to a computational mesh, on which CFD analysis will be performed (usually using finite-element or finite-volume methods). Input to the calculations in the form of two-point pressure or, more usually, one-point flow-rate wave forms also needs to be measured. Again, MR methods are increasingly being used for flow rate measurement, though Doppler ultra-sound is currently more reliable. At present every stage of this process has problems and raises doubts about its validity and accuracy. Nevertheless, the development of such integrated approaches is an area of great current excitement, and I am sure that we will soon see reliable data emerging routinely for clinical use with individual patients: but it will be expensive in computer resources. See [46], especially pages 717–728, and [47] for some recent abstracts in this area. On the basis of the definition given at the start of this paper, such fully computational approaches can be classified as non-mathematical.

The second approach is that of the applied mathematician: examine in great thoroughness highly idealised geometries which can be readily reproduced by other investigators and in each of which a single physical mechanism or phenomenon is exemplified. The main example chosen for further investigation in Section 3.2 below is that of steady or pulsatile flow in a

uniform curved tube with circular cross-section. Another example is that of unsteady, high-Reynolds-number flow in a straight tube of non-uniform cross-section. A two-dimensional version of the problem is discussed fully in [10, Section 4]. While being simple enough for mathematical treatment, using the sophisticated methods of interactive boundary-layer theory pioneered by Smith [48, 49], the analysis has revealed some novel phenomena which may be significant in the arterial context and which are certainly of great fluid mechanical interest. Many of the phenomena were first observed experimentally [50, 51] but were confirmed computationally [52, 53] and analytically. For example, steady flow past an asymmetric, oscillating indentation leads to the generation of vorticity waves downstream with wavelength $O(a\text{Re}^{1/7})$ where a is the undisturbed channel with and Re is the (large) Reynolds number, if the Strouhal number ($\omega a/\overline{U}$, where ω is frequency and $\overline{U}$ mean velocity) is $O(\epsilon\text{Re}^{-1/7})$, ϵa being the indentation amplitude. Beneath the crests and above the troughs of these (large-amplitude) waves are regions of flow recirculation, *i.e.*, separated eddies, but instead of being very sluggish, as in steady separated eddies, the flow in these eddies is very rapid, and the local wall shear stress has a much higher value than elsewhere, not much lower. Similar vorticity waves are found for oscillatory flow past a fixed asymmetric indentation, but in that case there is no simple theory to predict them. In both cases, however, regions of flow separation appear at significant distances from the geometrical disturbance that gives rise to them, but in those regions the WSS is large not small. Neither of these features could be predicted from a knowledge of steady separated flow. Moreover, it should be remembered that steady flow in a diverging channel is non-unique at large Reynolds number, even when the divergence is sufficiently gradual for boundary-layer theory to be applicable everywhere [54, 55]. It is not yet known whether all these features carry over to three dimensions and hence to arteries, but it is clear that steady-flow intuition cannot be trusted.

3.2. FLOW IN CURVED TUBES

3.2.1. *Steady, fully-developed flow*

When viscous fluid flows steadily in a uniform curved tube of radius a and centre-line radius of curvature R, the flow is not everywhere parallel to the curved centreline: a secondary motion appears even at low values of the Reynolds number. This is because a lateral pressure gradient is needed to cause the flow to change direction and, in response, the faster-moving fluid near the centre of the tube moves in a curve with larger radius of curvature than the slower-moving fluid near the walls. Thus the centre fluid is swept towards the outside of the bend while the fluid near the wall moves towards the inside. In a tube of small curvature ratio $\delta = a/R$ it can be readily shown that the steady, fully-developed (independent of axial coordinate) flow depends on a single dimensionless parameter

$$D = (2\delta)^{1/2}\hat{G}a^3/\mu\nu, \tag{15}$$

where $\hat{G}$ is the pressure gradient and μ, ν are the fluid's dynamic and kinematic viscosities; this is $(2\delta)^{1/2}$ times the Reynolds number in a straight pipe. D is usually called the Dean number because Dean [56] was the first to analyse such flow, expanding the velocity field in powers of D (actually in powers of $D/96$, so the solution's validity is not limited to values of D much less than 1.) Secondary flows such as those predicted by Dean are routinely seen experimentally.

Later authors have provided either numerical or approximate analytical solutions to Dean's equations (*i.e.*, the small-δ version of the Navier-Stokes equations) for values of $D/96$ that are
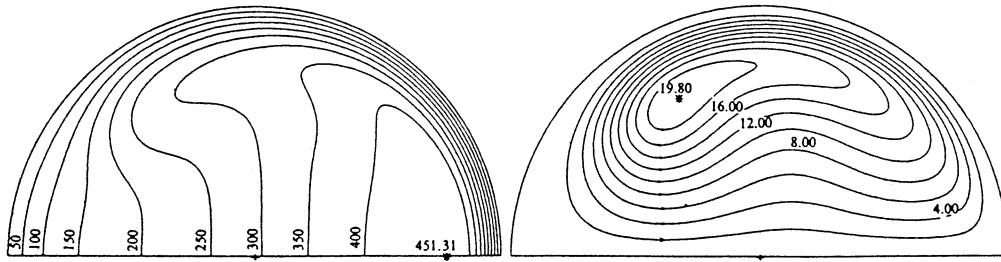
Figure 5. Computed axial velocity contours (left) and two-vortex secondary flow streamlines (right) for steady flow in a curved tube of small curvature at $D = 5000$. (From [64], with permission.)

not small or $O(1)$. For example, Collins and Dennis [57] gave solutions for values of D up to 5000, and were able to show that, as D is increased, the secondary motion causes an increasing displacement of the peak longitudinal velocity towards the outside of the bend, where there is therefore a high wall shear, and also pulls relatively high velocities round the side walls, so that the longitudinal velocity profile in a plane perpendicular to the plane of curvature becomes M-shaped (Figure 5). The changed axial flow also distorts the secondary flow, but the basic Dean picture remains. For large D, Ito [58] indicated how an asymptotic expansion could proceed, with an inviscid but vortical core flow in which the axial velocity $\hat{w}$ and the transverse stream function $\hat{\Psi}$ are given by

$$\hat{w} = \frac{\nu}{a}(2\delta)^{-1/2}D^{2/3}f(x), \quad \hat{\Psi} = \nu D^{1/3}y/f'(x) \tag{16}$$

where x, y are the dimensionless transverse coordinates (with $y = 0$ on the plane of symmetry) and $f(x)$ is an arbitrary function, presumably to be determined from matching to the viscous boundary layer on the tube wall, $r = (x^2+y^2)^{1/2} = 1$. Ito also showed that this boundary layer would have dimensionless thickness $D^{-1/3}$, and gave a crude (Kármán-Pohlhausen) approximation to the solution of the boundary-layer equations and the function $f(x)$. However, Ito noted, and Dennis and Riley [59] confirmed, that the boundary-layer approximation breaks down near the innermost point on the curved wall ($y = 0$, $x = -1$), and a satisfactory resolution of this problem has not yet been proposed. Certainly, the numerical solutions of Collins and Dennis [57] appeared to be consistent with Ito's asymptotic structure, so it might be supposed that that structure holds everywhere, except perhaps in a neighbourhood of the innermost point.

This was the position when two reviews of flow in curved tubes appeared in the early 1980s: Pedley [9, Chapter 4] and Berger *et al.* [60]. The only real doubt about the asymptotic structure had been cast by Van Dyke [61], who analysed the problem using his technique of extending the validity of series expansions (here, in powers of D) to large values of the parameter by a suitable transformation. He concluded that at least one branch of the large D solution – the analytic continuation of the Dean expansion – had a different structure, in which (for example) the transverse stream-function $\hat{\Psi}$ was proportional to $\nu D^{1/4}$. No direct asymptotic study has yet confirmed the existence of a solution with this structure; if it existed, it would suggest that the large D flow is non-unique, with at least two different solution structures.

During the 1980s a sequence of papers appeared in which such non-uniqueness was clearly demonstrated computationally [62–64]. When D is sufficiently small, the steady-flow equations have just one solution and there is a single secondary-flow vortex in each half of the tube, as found by Dean [56] and by Collins and Dennis [57]. Dennis and Ng [62] found
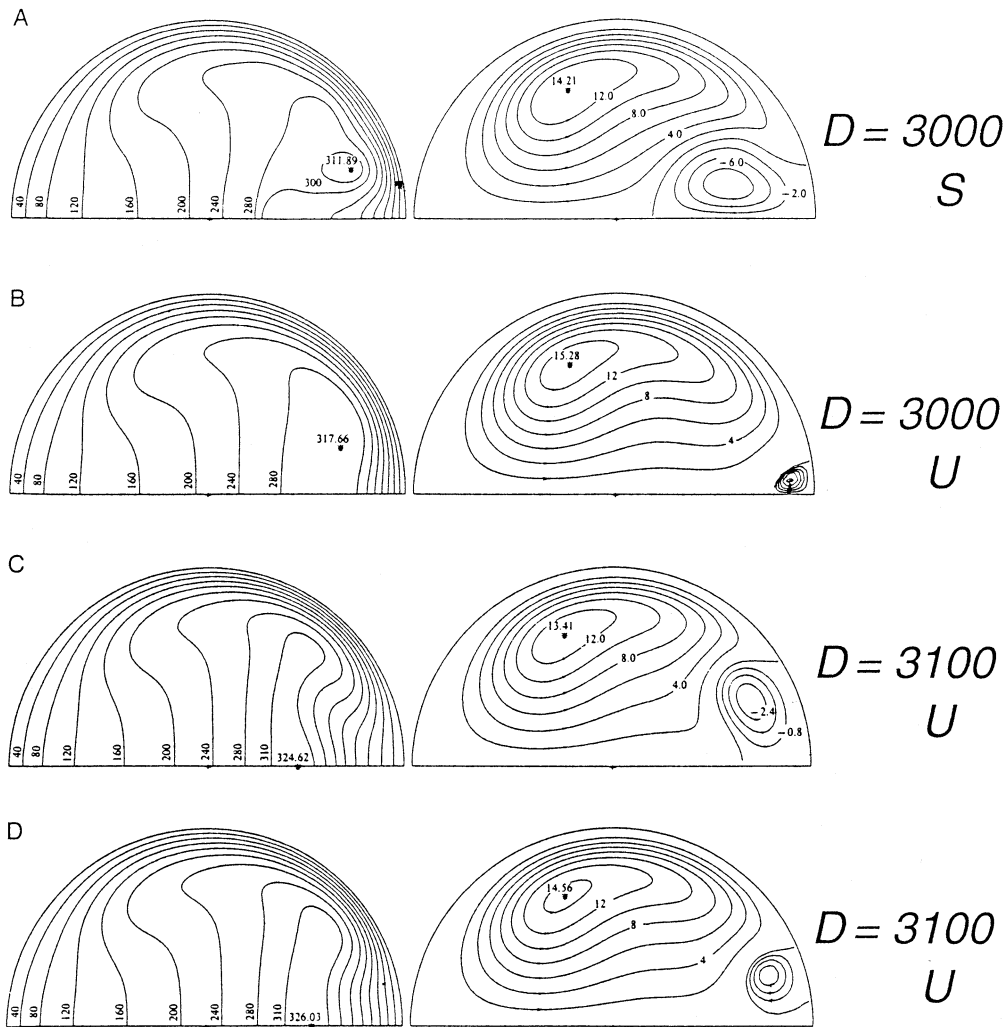
Figure 6. Computed axial velocity contours (left) and secondary flow streamlines (right) for steady flow in a curved tube of small curvature at comparable values of the Dean number, D, showing the non-uniqueness of the flow. The flow marked S is stable, those marked U are unstable. (From [64], with permission.)

that a continuous branch of such two-vortex flow persists to high values of D (with a flow structure that varies with D in a manner consistent with Ito's [58] proposal, not Van Dyke's [61] suggestion). However, they also found that there is a critical value of D, say D_1, above which more than one steady solution to the equations exists; Dennis and Ng [62] found D_1 to be about 956, a value confirmed by both Daskopoulos and Lenhoff [64] and Yanase *et al.* [63]. Daskopoulos and Lenhoff computed two more solutions for D in excess of D_1, and two more again for D greater than another critical value D_2 (approximately 2500). The contour and streamline plots for all four solutions are shown in Figure 6 of which A and B are the two solutions that exist for $D > D_1$ (at $D = 3000$) and C and D are those that exist only for $D > D_2$ (at $D = 3100$). All these solutions are four-vortex in character (two vortices in each half of the tube) and do not look very different from each other. However, Daskopoulos and Lenhoff investigated their stability, and found that the only stable four-vortex flow for

$D > D_1$ is that depicted in Figure 5(a); the others are all unstable. This result suggests that, for $D > D_1$, the flow that will actually be observed in an experiment will be either the two-vortex solution or the four-vortex solution such as that of Figure 5(b). Presumably, if the Dean number is gradually increased from a low value, the two-vortex flow will persist, but a suitably violent perturbation could result in the four-vortex flow being set up.

We should note that Yanase *et al.* [63] performed a more general stability analysis, not restricted to disturbances with top-bottom symmetry, and concluded that the four-vortex flow is unstable after all, and therefore not observable. In contrast, in the experiments of Cheng and Mok [65], the four-vortex flow was observed, and hence presumably stable, for a range of values of Dean number when the curvature ratio δ was not very small.

It may be thought that whether a unique, stable steady flow exists for a certain geometry and Reynolds (or Dean) number is not particularly important when the real flows of interest are time-dependent anyway. Starting from a given initial state, with a given time-dependent pressure gradient, surely the flow will be well determined as a solution of the Navier-Stokes equations? In principle that is correct, but the existence of more than one steady solution, stable or unstable, means that the outcome can depend very sensitively on the initial or boundary conditions. A small change in geometry, or a small change in the pressure-gradient waveform, may lead to a substantially different pattern of flow and wall shear. The pattern could vary from one cycle to the next, in a chaotic manner.

3.2.2. *Unsteady, fully-developed flow*

Apart from the stability analyses referred to above, there have been essentially two types of unsteady flow studied, oscillatory and impulsively-started. Oscillatory flows include those with non-zero and zero mean pressure gradient (or flow rate) as well as those with non-sinusoidal time dependence, *e.g.* mimicking the physiological pressure-gradient wave form, as well as sinusoidal. Principal papers include that of Lyne [66], who analysed the transverse steady streaming generated within the Stokes boundary layers driven by a sinusoidally oscillating pressure gradient (zero mean); he found a two-vortex steady-streaming flow, directed in the opposite sense to steady secondary flows. Smith [67] analysed many different regimes and Blennerhassett [68] looked in particular at the most interesting case, in which the magnitude of the Lyne steady-streaming velocity associated with the oscillatory part of the pressure gradient is of comparable magnitude to the secondary flow that would be driven by the mean pressure gradient if that were acting alone. Blennerhassett found bifurcations to non-uniqueness for a range of values of the mean Dean number D if the "steady-streaming Reynolds number" R_s exceeds a critical value between 75 and 100 ($R_s = \delta \hat{W}_a^2 / \Omega \nu$, where $\hat{W}_a$ is the axial core velocity amplitude and Ω is the oscillation frequency). When R_s exceeds about 150 the range of values of D for which non-uniqueness is found seems to extend to infinity. These findings were described and discussed in more detail by Pedley [9]. There have been more recent computational studies of unsteady flow in curved tubes (*e.g.* [69, 70]), but apart from demonstrating the complexity of the flow and its variability between different regions of parameter space, these do not reveal any feature of particular interest to the mathematical modeller.

Flow in a curved tube driven by an impulsively-started (and then constant) pressure gradient can be regarded as a model (though not a very good one) for flow in the aortic arch at the start of systole. The inviscid core flow is that of a potential vortex with axis at the tube's centre of curvature and therefore with higher velocity and hence wall shear stress towards the inside of the bend. However, the associated pressure gradient drives a secondary flow in the boundary layers from outside to inside, so the boundary layer thickens more rapidly at the

inside and the site of maximum WSS switches to the outside after a short time. Farthing [71] performed a power-series expansion of the flow for small times, but it clearly broke down a little while after the switch in position of maximum WSS. The reason for the breakdown lies in the collision of the two secondary flows (top and bottom) at the innermost point and the consequent explosive thickening of the boundary layers. The nature of the resulting singularity has been elegantly analysed by Lam [72] and by Riley [73], using Lagrangian and Eulerian methods, respectively. Unfortunately, however, knowing the nature of the breakdown does not help one analyse the structure of the flow afterwards. For that we would have to rely on computational simulation or experiment.

In fact directly relevant experiments, and computations, have been performed by a group at Marseille [74]. Starting flow was generated gravitationally in a large U-tube of circular cross-section and the developing secondary flow was visualised using injected fluorosceine, illuminated by a transverse laser sheet at various axial locations. At positions unaffected for some time by the straight inlet and outlet regions (the flow therefore being fully developed for that time) the collision of the secondary-flow boundary layers at the inner wall was clearly seen. As the flow then erupted from the boundary layer a transverse vortex pair was formed, with the appearance of a mushroom, which propagated across the cross-section. For some parameter values the secondary vortex pair eventually filled the cross-section, as in fully-developed steady flow, but for others the propagation stopped partway.

3.2.3. *Entry flow*

In finite or non-uniform tubes the flow cannot be fully-developed and must depend on the axial coordinate, s (here made non-dimensional with respect to tube radius a). A number of authors, starting with Olson [75] experimentally and Singh [76] mathematically, have investigated entry flow, in which an irrotational, nearly flat, velocity profile exists at the entrance $s = 0$. Very near the entrance, Blasius-type boundary layers develop, of thickness proportional to $(s/\mathrm{Re})^{1/2}$. However, the curvature-induced transverse pressure gradient initiates secondary motions, as for the unsteady flow considered above. Eventually boundary-layer theory breaks down at the inside of the bend, after a distance $s = O(\delta^{-1/2})$, because the secondary flows collide, in a singular manner first elucidated by Stewartson *et al.* [77]. Thereafter the coreflow is distorted and fully-developed flow eventually emerges; the details are susceptible only to computational and experimental investigation. The distance required to establish fully-developed flow is shorter in a curved tube than a straight tube, because advection of vorticity and momentum by the secondary flow is more efficient at redistributing them than viscous diffusion alone. In a straight tube the entry length is proportional to a Re; in a curved tube the corresponding quantity is $a\mathrm{Re}^{1/2}\delta^{-1/4}$ for $\delta \ll 1$ (or, equivalently, $aD^{1/3}\delta^{-1/2}$ from Equations (15–16) – see Yao and Berger [78]).

Unsteady, non-reversing entry flow is quasi-steady very near the inlet, where the boundary layer is so thin that the flow responds effectively instantaneously to changes in the longitudinal pressure gradient. The quasi-steady Blasius boundary-layer solution can thus be used as the leading term of an expansion in powers of s, suitably modified by curvature and time dependence, as demonstrated by Pedley [9, Section 4.4]. For a straight tube, Pedley [79] gave an approximate analysis of the transition from quasi-steady Blasius flow near the entrance to a purely diffusive Rayleigh layer further downstream, all within the confines of boundary-layer theory. However, as for steady flow, such boundary layer theory breaks down an $O(1)$ distance from the entrance in a curved tube, owing to the collision of the secondary-flow boundary layers, and we do not have a complete solution for the flow further downstream.

3.2.4. *Variable curvature*

Arteries are not simple curved tubes of uniform, constant curvature. Most vessels have non-uniform curvature and, indeed, non-planar curvature; extramyocardial coronary arteries, in addition, have time-dependent curvature since the dimensions of the heart, on whose surface they lie, vary considerably during a single cardiac cycle. All these features have been studied in recent years; the most complete simulations have come from direct computation, as usual, but the first papers in each case have had a substantial mathematical component, as the authors have tried to understand the basic physics of a new sub-branch of fluid dynamics that had not arisen previously in another context.

The first relevant study was that by Smith [80] who analysed steady flow from a straight tube (in $s < 0$, say) in which there is Poiseuille flow, into a curved tube of small, constant curvature δ (in $s > 0$). The analysis required a three-dimensional version of the internal boundary-layer theory developed for indented channels [48, 49], which is quite complex. The overall results are not very surprising, in that, near $s = 0$, the core flow goes straight on, generating rather strong secondary boundary layers as it impinges on the wall of the curved tube. There is also an upstream influence, due to the pressure perturbation induced by the impingement, and the flow in the boundary layer adjusts itself accordingly over a distance comparable with the tube radius. Downstream, as usual, the solution breaks down at $s = O(1)$, where the perturbation to the oncoming flow can no longer be regarded as small.

Smith's solution was (slightly) extended by Pedley [9, Section 4.5] to permit continuous variation with s of the curvature parameter δ: the tube has uniform, circular cross-section, but the (planar) curvature varies. The essential modification was to incorporate $\delta(s)$ into the coordinate system, so that the boundary of the tube in every constant $-s$ plane, perpendicular to the centre line, is always at $r = 1$ in polar coordinates (r, θ). A further extension to space- *and* time-dependent (but still planar) curvature was made by Lynch *et al.* [81]. Again, the object was to keep the boundary at $r = 1$, by incorporating the variable dimensionless curvature $\delta(s, t)$, so that the leading term in any new solution would be a known solution, such as Poiseuille flow in a straight tube or flow in a uniform, fixed, curved tube, and would be valid for all s. This aim was achieved, but the resulting equations were extremely complex. For example, the θ-component of the Navier-Stokes equation is as follows:

$$
\upsilon_t + u\upsilon_r + \frac{1}{r}\upsilon\upsilon_\theta + \frac{1}{h}w\upsilon_s + \frac{1}{r}u\upsilon - \frac{af_{ss}\sin\theta}{C\,h}w^2
$$

$$
- \frac{2af_{st}}{C}\sin\theta\,w - a\left[f_{tt}C - af_s I_{tt}\right]\sin\theta
$$

$$
+ \frac{a^2r}{C^2}f_{st}^2\sin\theta\cos\theta
$$

$$
= -\frac{1}{r\rho}p_\theta + \nu\left\{\upsilon_{rr} + \frac{1}{h^2}\upsilon_{ss} - \frac{1}{rh}w_{\theta s} - \frac{1}{r}u_{r\theta}\right.
$$

$$
+ \frac{1}{r^2h}u_\theta - \frac{1}{r^2h}\upsilon - \frac{af_{ss}}{Ch}\cos\theta\upsilon_r
$$

$$
- \frac{a}{Ch^3}\left[f_{sss} + \frac{a^2f_sf_{ss}^2}{C^2}\right][\sin\theta\,w - r\cos\theta\upsilon_s]
$$

$$
+ \frac{1}{r}\upsilon_r - \frac{af_{ss}}{Ch^2}\sin\theta\,w_s - \frac{2a}{Ch}\sin\theta\left[f_{sst} + a^2\frac{f_sf_{ss}f_{st}}{C^2}\right]\right\},
$$

where s is distance measured along the tube centreline, which lies in the $x - y$ plane and has equation

$$y = af(s, t);$$

also

$$h = 1 - \frac{arf_{ss}}{C} \cos\theta, \quad C = \left(1 - a^2 f_s^2\right)^{1/2}.$$

It is clear that a set of equations like this can be solved analytically only in certain asymptotic limits in which many of the terms drop out. Lynch *et al.* [81] looked in particular at two cases. One was a uniformly curved tube with small but weakly time-dependent curvature (a perturbation to Dean flow). The other was a time-dependent sinuous tube of small amplitude (an extension to the steady flow analysed by Murata *et al.* [82]. The results were of some interest though not very surprising. For example, in a sinuous tube oscillating at high frequency the axial wall shear stress is greatest at the inside of bends, not the outside as in steady flow, because the core flow goes essentially straight on all the time, and the boundary layer will be thinnest at the inside. However, the main value of these asymptotic solutions is as test cases for full computations.

It will be clear from the above that, in the author's opinion, a judicious mixture of mathematical modeling, computation and experiment is capable of providing a much greater depth of understanding of fluid mechanical phenomena than either of the last two on their own, or even together. The uninitiated might think that the value of mathematical modelling is greatest in the early years of a field, such as arterial fluid mechanics, and all the details can later be filled in by computer, but that is not the case. To underline the fact that the modelling approach is by no means dead, Section 4 is devoted to a recent model by Waters [7, 8] of transmyocardial laser revascularisation.

4. Transmyocardial laser revascularisation (TLR)

As stated in the introduction, this procedure consists of using a laser to drill a number of tunnels, of around 1mm in diameter, partway through the wall of the left ventricle from the inside, when that part of the wall has been deprived of blood supply as a result of an infarct. The idea is that the heart muscle can be perfused with blood from these tunnels, and kept alive long enough for angiogenesis to have generated a new network of capillaries emanating either from the tunnels or from other, unblocked, parts of the coronary circulation. The hypothesis that forms the basis of the mathematical model of Waters [7, 8] is that the pulsation in the dimensions of the tunnels, driven by the beating of the ventricle, causes blood to be pumped in and out of them. Oxygen uptake is enhanced over what would be achieved by diffusion alone by a process of shear (or Taylor) dispersion in the tunnels. The purpose of the modelling is to estimate the degree of that enhancement.

The tunnels are assumed to be sufficiently far apart not to influence each other, so that a single tunnel can be studied in isolation. This tunnel is taken to be a long, narrow cylinder of time-varying length and radius (Figure 7). Blood, modelled as a viscous, incompressible Newtonian fluid, occupies and flows in the tunnel. The oxygen concentration in the tunnel is $C(\boldsymbol{x}, t)$, It is taken up by the tissue across the wall of the tunnel; in the tissue, where its concentration is $\theta(\boldsymbol{x}, t)$, it is consumed, at a rate proportional to its concentration. We take cylindrical polar coordinates (x, r), which have been non-dimensionalised with respect to the
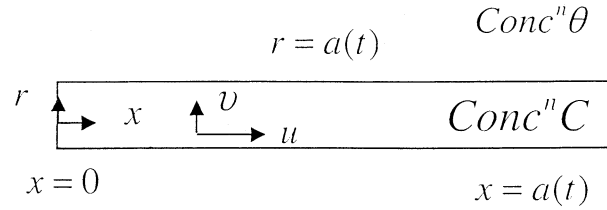
Figure 7. Sketch of the closed-end tunnel drilled in the left ventricle wall during transmyocardial laser revascularisation. All variables shown are dimensionless: cylindrical polar coordinates (x, r), velocity components (u, v), oxygen concentration in blood (C) and tissue (θ), length and radius of the tunnel $(a(t)$, where t is time).

resting length b_0 and radius a_0 of the tunnel, respectively $(b_0 \gg a_0)$. The time-dependent length and radius are then given by

$$x = a(t) \quad \text{and} \quad r = a(t), \quad \text{where} \quad a(t) = 1 + \epsilon \sin t \tag{17}$$

and where time t is non-dimensionalised with respect to the inverse of the radian frequency of the oscillation, $1/\omega$, and ϵ is a small amplitude parameter. The closed end of the tunnel is at $x = 0$.

As the tunnel expands, blood is sucked in at $x = a(t)$; as it contracts, the blood is pushed out again. Conservation of mass means that the dimensionless longitudinal velocity u is directly proportional to x, and the radial velocity v is a function only of r and t, except in small regions near the ends. Hence the nonlinear inertia terms in the x-component of the Navier-Stokes equation, such as uu_x, will be non-zero, so the velocity field cannot vary purely sinusoidally in time. For example, if u were supposed to be sinusoidal – proportional to $\epsilon x \cos t$, say – then uu_x would be proportional to $\epsilon^2 x \cos^2 t$, which has non-zero mean. The non-zero mean flow generated by such nonlinear self-interaction of an oscillating component is the *steady streaming*. The steady streaming is partly, but not wholly, responsible for the enhancement of oxygen transfer, as we shall see.

In the tube, the oxygen concentration C, scaled with the mean concentration in the blood, obeys the dimensionless advection-diffusion equation

$$C_t + \boldsymbol{u} \cdot \nabla C = \frac{\epsilon^2}{P} \nabla^2 C, \tag{18}$$

where the oscillatory Peclet number is assumed to be large, of $O(\epsilon^2)$ as $\epsilon \to 0$:

$$\frac{a_0^2 \omega}{D} = \frac{P}{\epsilon^2} \gg 1. \tag{19}$$

The velocity field can be expanded in powers of ϵ, with the purely sinusoidal oscillation as the leading term, so that

$$\boldsymbol{u} = \epsilon \boldsymbol{u}_1 + \epsilon^2 \boldsymbol{u}_2 + \dots, \tag{20}$$

where

$$\boldsymbol{u}_1 = \Re e \left(\boldsymbol{u}_{11} e^{it} \right)$$
$$\boldsymbol{u}_2 = \boldsymbol{u}_{20} + \Re e \left(\boldsymbol{u}_{22} e^{2it} \right).$$

Here the quantities $\boldsymbol{u}_{ij}$ are functions only of position, $\boldsymbol{u}_{20}$ representing the steady streaming, and $\boldsymbol{u}_{11}, \boldsymbol{u}_{22}$ being complex and representing the oscillations.

Substitution of (20) in (18) suggests that C also be expanded in powers of ϵ:

$$C(\boldsymbol{x}, t) = C_0 + \epsilon C_1 + \epsilon C_2.$$

At leading order in ϵ, (18) gives $\partial C_0 / \partial t = 0$, so we can deduce that C_0 is a function only of $\boldsymbol{x}$, but nothing further. First order in ϵ then gives

$$C_{1t} = -\boldsymbol{u}_1 \cdot \nabla C_0 = -\frac{1}{2}\left(\boldsymbol{u}_{11}e^{it} + \boldsymbol{u}_{11}^*e^{-it}\right) \cdot \nabla C_0,$$

where * represents complex conjugate. Hence

$$C_1 = \frac{i}{2}\left(\boldsymbol{u}_{11}e^{it} - \boldsymbol{u}_{11}^*e^{-it}\right) \cdot \nabla C_0.$$

The $O(\epsilon^2)$ equation is

$$C_{2t} + \boldsymbol{u}_1 \cdot \nabla C_1 + \boldsymbol{u}_2 \cdot \nabla C_0 = \frac{1}{P}\nabla^2 C_0,$$

and it can be seen that the time-average of this equation gives a single equation for $C_0(\boldsymbol{x})$. After some calculation we obtain

$$\boldsymbol{U} \cdot \nabla C_0 = \frac{1}{P}\nabla^2 C_0, \tag{21}$$

where

$$\boldsymbol{U} = \frac{1}{2}\Im m(\boldsymbol{u}_{11} \cdot \nabla \boldsymbol{u}_{11}^*) + \boldsymbol{u}_{20}.$$

That is to say, the mean oxygen concentration in the tube satisfied a steady advection-diffusion equation, but with an effective velocity field $\boldsymbol{U}$ that differs from the actual mean velocity $\boldsymbol{u}_{20}$. That is the most interesting mathematical feature of this model.

In the present case we can write

$$\boldsymbol{U} = [xU(r), V(r)]$$

where U, V can be calculated analytically. Moreover the modified Peclet number P is, in practice, quite small. It can then be shown that the blood-oxygen concentration, averaged across the tunnel cross-section, $\hat{C}$, satisfies a simple ordinary differential equation in x:

$$x^2\frac{\partial^2 \hat{C}}{\partial x^2} + 2x\frac{\partial \hat{C}}{\partial x} - \gamma \hat{C} = 0 \tag{22}$$

where γ is proportional to P^{-2} but also depends on the oxygen diffusivity and consumption rate in the tissue, and its transfer rate across the tunnel wall.

From the solution of this equation, subject to appropriate boundary conditions at the ends, the mean oxygen uptake rate by the tissue as a whole can be computed. Quantitatively, the results are not startling but, based on values of the transfer rate and consumption rate obtained from the literature (in the case of transfer rate, not from coronary blood vessels), Waters predicted that an array of tunnels of diameter 1mm, spaced 4mm apart, would provide an oxygen uptake rate of $5 - 10 \times 10^{-10}$mol cm^{-3} s^{-1}. This is still only 1–2% of the rate for healthy heart muscle, but exceeds that obtained in static tunnels, by pure diffusion, by a factor of 10–20.

Appendix A. The effect of aging on the phase difference between the pressure and flow-rate waveforms in the aorta

Following Pedley [10, Section 3.3], we suppose that the pressure wave incident on a bifurcation of an elastic tube has the sinusoidal form

$$P_I \cos\left[\omega(t - x/c_1)\right],$$

where c_1 is the wave speed in the parent tube, ω is frequency and P_I is amplitude. We take $x = 0$ at the bifurcation, so $x < 0$ in the parent tube. Then the full pressure and flow-rate in the parent tube, relative to the constant mean pressure, are given by linear, long-wavelength theory to be

$$\frac{P}{P_I} = \cos\left[\omega\left(t - \frac{x}{c_1}\right)\right] + \beta \cos\left[\omega\left(t + \frac{x}{c_1}\right)\right], \tag{A1}$$

$$\frac{Q}{Y_1 P_I} = \cos\left[\omega\left(t - \frac{x}{c_1}\right)\right] - \beta \cos\left[\omega\left(t + \frac{x}{c_1}\right)\right], \tag{A2}$$

where

$$\beta = \frac{Y_1 - (Y_2 + Y_3)}{Y_1 + (Y_2 + Y_3)} \tag{A3}$$

and Y_j is the characteristic admittance of tube j (1 = parent, 2,3 = daughters).

For a given value of $x < 0$, we calculate the times τ_1/ω, τ_2/ω at which p and Q, respectively, are maximum. Simple calculus gives

$$\tan \tau_1 = -\gamma \tan \alpha, \quad \tan \tau_2 = -\gamma^{-1} \tan \alpha$$

where $\alpha = -\omega x/c_1 > 0$ and

$$\gamma = \frac{1 - \beta}{1 + \beta} > 0.$$

Hence

$$\tan(\tau_1 - \tau_2) = \frac{\gamma^{-1} - \gamma}{2} \sin 2\alpha = \frac{2\beta}{1 - \beta^2} \sin 2\alpha. \tag{A4}$$

Thus, if $0 < \beta < 1$ and if $0 < \alpha < \pi/4$, and presuming that $\tau_1 - \tau_2$ takes the smallest positive value given by (A4), it follows that $\tau_1 - \tau_2$ deceases as α decreases. However, if $0 < \beta < 1$ and $\pi/4 < \alpha < \pi/2$, $\tau_1 - \tau_2$ will increase as α decreases.

In applying this to the pressure and flow-rate pulses in the aorta, we recall that the aortic bifurcation is normally a site of positive pressure-wave reflection, *i.e.*, $0 < \beta < 1$. We also note that $\alpha/2\pi$ is the distance upstream from the bifurcation as a fraction of the pulse wavelength. For a frequency of 1Hz and a wave speed of 5–8 ms^{-1}, the wavelength is 5–8m, so near the aortic valve, where $-x$ is the length of the aorta, say about 1m, α would be in the range $\pi/4 < \alpha \lesssim 2\pi/5$. Thus, finally, if the only effect of aging is to stiffen the arteries – *i.e.*, to increase c_1, c_2 and c_3 equally – without altering the area ratio at the bifurcation so that β would remain unchanged, we may conclude that $\tau_1 - \tau_2$ would increase with age.

Acknowledgements

References

1. T.J. Pedley, James Lighthill and his contributions to fluid mechanics. *Annu. Rev. Fluid Mech.* 33 (2001) 1–41.
2. J. Lighthill, *Mathematical Biofluiddynamics.* Philadelphia: SIAM (1975) 281 pp.
3. C.G. Caro, J.M. Fitz-Gerald and R.C. Schroter, Atheroma and arterial wall shear: observations, correlation and proposal of a shear dependent mass transfer mechanism for atherogenesis *Proc. R. Soc. London* B177 (1971) 109–159.
4. J. Lighthill, Physiological fluid dynamics: a survey. *J. Fluid Mech.* 52 (1972) 475–497.
5. J. Lighthill, Pressure-forcing of tightly fitting pellets along fluid-filled elastic tubes. *J. Fluid Mech.* 34 (1968) 113–143.
6. H. Tözeren and R. Skalak, The steady flow of closely fitting incompressible elastic spheres in a tube. *J. Fluid Mech.* 87 (1978) 1–16.
7. S.L. Waters, Solute uptake through the walls of a pulsating channel. *J. Fluid Mech.* 433 (2001) 193–208.
8. S.L. Waters, A mathematical model for the laser treatment of heart disease. *ASME J. Biomech. Engng.* (2003) (in press).
9. T.J. Pedley, *The Fluid Mechanics of Large Blood Vessels.* Cambridge: Cambridge University Press (1980) 446 pp.
10. T.J. Pedley, Blood flow in arteries and veins. In: G.K. Batchelor, H.K. Moffatt and M.G. Worster (eds.), *Perspectives in Fluid Dynamics.* Cambridge: Cambridge University Press (2000) pp. 105–158.
11. T. Young, On the functions of the heart and arteries. *Phil. Trans. R. Soc. London* 99 (1809) 1–31.
12. M.G. Taylor, The input impedance of an assembly of randomly branching elastic tubes. *Biophys. J.* 6 (1966) 29–51.
13. W.R. Milnor, *Hemodynamics*, 2nd ed. Baltimore: Williams and Wilkins (1989) 419 pp.
14. J.R. Womersley, Method for the calculation of velocity, rate of flow and viscous drag in arteries when the pressure gradient is known. *J. Physiology* 127 (1955) 553–563.
15. J.R. Womersley, The mathematical analysis of the arterial circulation in a state of oscillatory motion. *Wright Air Development Center Technical Report* WADC-TR (1957) pp. 56–614.
16. D.A. McDonald, *Blood Flow in Arteries.* London: Edward Arnold (1974) 496 pp.
17. M.B. Histand and M. Anliker, Influence of flow and pressure on wave propagation in the canine aorta. *Circulation Res.* 32 (1973) 524–529.
18. W.R. Milnor and C.D. Bertram, The relation between arterial viscosity and wave propagation in the canine femoral artery in vivo. *Circulation Res.* 43 (1978) 870–879.
19. C.D. Bertram, Energy dissipation and pulse wave attenuation in the canine carotid artery. *J. Biomech.* 13 (1980) 1061–1073.
20. C.H. Smit, On the modelling of distributed outflow in one-dimensional models of arterial blood flow. *Zeitschr. angew. Math. Physik* 32 (1981) 408–420.
21. M. Anliker, R.L. Rockwell and E. Ogden, Nonlinear analysis of flow pulses and shock waves in arteries, I and II. *Zeitschr. angew. Math. Physik* 22 (1971) 217–246 and 563–581.
22. J.H. Gerrard and L.A. Taylor, Mathematical model representing blood flow in arteries. *Med. Biolog. Engng. Comp.* 15 (1977) 611–617.
23. R. Holenstein, P. Niederer and M. Anliker, A viscoelastic model for use in predicting arterial pulse waves. *ASME J. Biomech. Engng.* 102 (1980) 318–325.
24. R. Chadwick, Pulse-wave propagation in an artery with leakage into small side branches. *Proc. Nat. Acad. Sciences USA* 82 (1985) 5237–5241.

25. J.K. Raines, *Diagnosis and Analysis of Atherosclerosis in the Lower Limb.* PhD thesis, Massachusetts Institute of Technology (1972).

26. M.S. Olufsen, A structured tree outflow condition for blood flow in the larger systemic arteries. *Amer. J. Physiology* 276 (1999) H257–H268.

27. T.J. Pedley, Nonlinear pulse wave reflection at an arterial stenosis. *ASME J. Biomech. Engng.* 105 (1983) 353–359.

28. S.J. Sherwin, V. Franke, J. Peiró and K. Parker, One-dimensional modelling of a vascular network in space-time variables. *J. Engng. Math.* 47 (2003) 217–250.

29. A. Quarteroni, S. Ragni and A. Veneziani, Coupling between lumped and distributed models for blood flow problems. *Comp. Visual. Sci.* 4 (2001) 111–124.

30. L. Formaggia, J.F. Gerbeau, F. Nobile and A. Quarteroni, On the coupling of 3D and 1D Navier-Stokes equations for flow problems in compliant vessels. *Comp. Meth. Appl. Mech. Engng.* 191 (2001) 561–582.

31. K.H. Parker, C.J.H. Jones, J.R. Dawson and D.G. Gibson, What stops the flow of blood from the heart? *Heart and Vessels* 4 (1988) 241–245.

32. K.H. Parker and C.J.H. Jones, Forward and backward running waves in the arteries: analysis using the method of characteristics. *ASME J. Biomech. Engng.* 112 (1990) 322–326.

33. C.J.H. Jones, K.H. Parker, R. Hughes and D.J. Sheridan, Nonlinearity of human arterial pulse wave transmission. *ASME J. Biomech. Engng.* 114 (1992) 10–14.

34. C.J.H. Jones, M. Sugawara, R.H. Davies, Y. Kondoh, K. Uchida and K.H. Parker, Arterial wave intensity: physical meaning and physiological significance. In: S. Hosoda, T. Yaginuma, M. Sugawara, M.G. Taylor and C.G. Caro (eds.), *Recent Progress in Cardiovascular Mechanics* Chur: Harwood (1994) pp. 129–148.

35. A.W. Khir, A. O'Brien, J.S.R. Gibbs and K.H. Parker, Determination of wave speed and wave separation in the arteries. *J. Biomech.* 34 (2001) 1145–1155.

36. F. Pythoud, N. Stergiopoulos and J.-J. Meister, Separation of arterial pressure wave into their forward and backward running components. *ASME J. Biomech. Engng.* 118 (1996) 295–301.

37. J. Lighthill, *Waves in Fluids.* Cambridge: Cambridge University Press (1978) 504pp.

38. J.-J. Wang, A.B. O'Brien, N.G. Shrive, K.H. Parker and J.V. Tyberg, Time-domain representation of ventricular-arterial coupling as a windkessel and wave system. *Amer. J. Physiology: Heart Circul. Physiology* 284 (2003) H1358–1368.

39. D.L. Fry, Acute vascular endothelial changes associated with increased blood velocity gradients. *Circulation Res.* 22 (1968) 165–197.

40. D.N. Ku, D.P. Giddens, C.K. Zarins and S. Glagov, Pulsatile flow and atherosclerosis in the human carotid bifurcation: positive correlation between plaque location and low and oscillating shear stress. *Arteriosclerosis* 5 (1985) 293–302.

41. P.F. Davies, Flow-mediated endothelial mechanotransduction. *Physiol. Rev.* 75 (1995) 519–560.

42. D.L. Fry, Mass transport, atherogenesis and risk. *Arteriosclerosis* 7 (1987) 88–100.

43. M.H. Friedman, Atherosclerosis research using vascular flow models: from 2-D branches to compliant replicas. *ASME J. Biomech. Engng.* 115 (1993) 595–601.

44. D.P. Giddens, C.K. Zarins and S. Glagov, The role of fluid dynamics in the localisation and detection of atherosclerosis. *ASME J. Biomech. Engng.* 115 (1993) 588–594.

45. T.J. Pedley, High Reynolds number flow in tubes of complex geometry with application to wall shear stress in arteries. In: C.P. Ellington and T.J. Pedley (eds.), *Biological Fluid Dynamics*, SEB Symposium no. 49. London: The Company of Biologists (1995) pp. 219–241.

46. V.K. Goel, R.L. Spilker, G.A. Ateshian and L.J. Soslowsky (eds.), *Proceedings of the 1999 Bioengineering Conference* (BED – Vol 42). New York: American Society of Mechanical Engineers (1999).

47. ASME, Proceedings of the 2001 Summer Bioengineering Conference, BIO'01 (2001).

48. F.T. Smith, Flow through constricted or dilated pipes and channels, Part I. *Q. J. Mech. Appl. Math.* 29 (1976) 343–364.

49. F.T. Smith, Flow through constricted or dilated pipes and channels, Part II. *Q. J. Mech. Appl. Math.* 29 (1976) 365–383.

50. T.J. Pedley and K.D. Stephanoff, Flow along a channel with a time-dependent indentation in one wall: the generation of vorticity waves. *J. Fluid Mech.* 160 (1985) 337–367.

51. I.J. Sobey, Observation of waves during oscillatory channel flow. *J. Fluid Mech.* 151 (1985) 395–426.

52. M.E. Ralph and T.J. Pedley, Flow in a channel with a moving indentation. *J. Fluid Mech.* 190 (1988) 87–112.

53. O.R. Tutty and T.J. Pedley, Oscillatory flow in a stepped channel. *J. Fluid Mech.* 247 (1993) 179–204.

54. L.R. Reneau, J.P. Johnston and S.J. Kline, Performance and design of straight, two-dimensional diffusers. *ASME J. Basic Engng* 89 (1967) 141–150.
55. M.S. Borgas and T.J. Pedley, Non-uniqueness and bifurcation in annular and planar channel flow. *J. Fluid Mech.* 214 (1990) 229-250.
56. W.R. Dean, The streamline motion of fluid in a curved pipe. *Phil. Mag.* (7) 5 (1928) 673–695.
57. W.M. Collins and S.C.R. Dennis, The steady motion of a viscous fluid in a curved tube. *Q. J. Mech. Appl. Math.* 28 (1975) 133–156.
58. H. Ito, Laminar flow in curved pipes. *Zeitschr. angew. Math. Physik* 49 (1969) 653–663.
59. S.C.R. Dennis and N. Riley, On the fully developed flow in a curved pipe at high Dean number. *Proc. R. Soc. London* A 434 (1991) 473–478.
60. S.A. Berger, L. Talbot and L.-S. Yao, Flow in curved pipes. *Annu. Rev. Fluid Mech.* 15 (1983) 461–512.
61. M. Van Dyke, Extended Stokes series: laminar flow through a loosely coiled pipe. *J. Fluid Mech.* 86 (1978) 129–145.
62. S.C.R. Dennis and M. Ng, Dual solutions for steady laminar flow through a curved pipe. *Q. J. Mech. Appl. Math.* 35 (1982) 305–324.
63. S. Yanase, N. Goto and K. Yamamoto, Dual solutions of the flow through a curved pipe. *Fluid Dyn. Res.* 5 (1989) 191–201.
64. P. Daskopoulos and A.M. Lenhoff, Flow in curved ducts: bifurcation structure for stationary ducts. *J. Fluid Mech.* 203 (1989) 125–148.
65. K.C. Cheng and S.Y. Mok, In: M. Herada (ed.), *Fluid Control and Measurement*, Vol. 2. New York: Pergamon (1986) pp. 765–773.
66. W.H. Lyne, Unsteady viscous flow in a curved pipe. *J. Fluid Mech.* 45 (1971) 13–31.
67. F.T. Smith, Pulsatile flow in curved pipes. *J. Fluid Mech.* 71 (1975) 15–42.
68. P. Blennerhassett, *Secondary Motion and Diffusion in Unsteady Flow in a Curved Pipe.* PhD thesis, Imperial College, London (1976).
69. S. Tada, S. Oshima and R. Yamane, Classification of pulsating flow patterns in curved pipes. *ASME J. Biomech. Engng.* 118 (1996) 311–317.
70. Y. Komai and K. Tanishita, Fully developed intermittent flow in a curved tube. *J. Fluid Mech.* 347 (1997) 263–287.
71. S.P. Farthing, Flow in the Thoracic Aorta and its Relation to Atherogenesis. PhD thesis, University of Cambridge (1977).
72. S.T. Lam, On High-Reynolds-Number Laminar Flows Through a Curved Pipe. PhD thesis, Imperial College, London (1988) 311 pp.
73. N. Riley, Unsteady fully-developed flow in a curved pipe. *J. Engng Math.* 34 (1998) 131–141.
74. A. Pascal-Mousselard and R. Pelissier, Secondary pattern in a bend for oscillatory and physiological flow conditions. In: Y. Matsuzaki, T. Nakamura and E. Tanaka (eds.), Abstracts of the Third World Congress of Biomechanics, Sapporo, Japan (1998) p.231.
75. D.E. Olson, Fluid mechanics relevant to respiration – flow within curved or elliptical tubes and bifurcating systems. PhD thesis, Imperial College, London (1971) 303 pp.
76. M.P. Singh, Entry flow in a curved pipe. *J. Fluid Mech.* 65 (1974) 517–539.
77. K. Stewartson, T. Cebeci and K.C. Chang, A boundary-layer collision in a curved duct. *J. Fluid Mech.* 33 (1980) 59–75.
78. L.-S. Yao and S.A. Berger, Entry flow in a curved pipe. *J. Fluid Mech.* 67 (1975) 177–196.
79. T.J. Pedley, Viscous boundary layers in reversing flow. *J. Fluid Mech.* 74 (1976) 59–79.
80. F.T. Smith, Fluid flow into a curved pipe. *Proc. R. Soc. London* A351 (1976) 71–87.
81. D.G. Lynch, S.L. Waters and T.J. Pedley, Flow in a tube with non-uniform, time-dependent curvature: governing equations and simple examples. *J. Fluid Mech.* 323 (1996) 237–265.
82. S. Murata, Y. Miyake and T. Inabe, Laminar flow in a curved pipe with varying curvature. *J. Fluid Mech.* 73 (1976) 735–752.